PAPER

Dynamic porous organic polymers with tuneable crosslinking degree and porosity†

Isabelle D. Wessely, ‡[a] Yannick Matt, ‡[ab] Qi An, ‡[c] Stefan Bräse [abd] and Manuel Tsotsalas *[ac]

Porous organic polymers (POPs) show enormous potential for applications in separation, organic electronics, and biomedicine due to the combination of high porosity, high stability, and ease of functionalisation. However, POPs are usually insoluble and amorphous materials making it very challenging to obtain structural information. Additionally, important parameters such as the exact molecular structure or the crosslinking degree are largely unknown, despite their importance for the final properties of the system. In this work, we introduced the reversible multi-fold nitroxide exchange reaction to the synthesis of POPs to tune and at the same time follow the crosslinking degree in porous polymer materials. We synthesised three different POPs based on the combination of linear, trigonal, and tetrahedral alkoxyamines with a tetrahedral nitroxide. We could show that modulating the equilibrium in the nitroxide exchange reaction, by adding or removing one nitroxide species, leads to changes in the crosslinking degree. Being able to modulate the crosslinking degree in POPs allowed us to investigate both the influence of the crosslinking degree and the structure of the molecular components on the porosity. The crosslinking degree of the frameworks was characterised using EPR spectroscopy and the porosity was determined using argon gas adsorption measurements. To guide the design of POPs for desired applications, our study reveals that multiple factors need to be considered such as the structure of the molecular building blocks, the synthetic conditions, and the crosslinking degree.

Various approaches to synthesise porous organic polymers (POPs)[1–3] and conjugated microporous polymers (CMPs)[4,5] have been developed to form extremely stable but at the same time highly porous solids based on simple organic building blocks.[6,7] The organic nature allows for functionalisation of the materials using organic chemistry, while the high porosity makes the active components accessible throughout the entire material.[8] The combination of high porosity, high stability, and ease of functionalisation results in the enormous potential of POPs for applications in separation, organic electronics, and biomedicine.[2,9–14] However, unlike the related covalent organic frameworks (COFs),[15–20] metal–organic frameworks (MOFs)[21,22] or porous coordination polymers (PCPs),[23] the synthesis of POPs

and CMPs is based on irreversible reactions, which leads to insoluble and amorphous materials and makes it very challenging to obtain structural information. Additionally, important parameters such as the exact molecular structure or the crosslinking degree are largely unknown, despite their unarguably large influence on the final properties of the system.[24,25]

To investigate the molecular structure of the organic linkers between the centres of two similar CMP materials, the group of Bunz and co-workers introduced molecular building blocks that were modified with digestible groups or cores, by substituting carbon with tin as the central atom.[24] This tin centre can be digested, resulting in molecular fragments of the frameworks, which were analysed using nuclear magnetic resonance (NMR) spectroscopy. The obtained fragments show a surprisingly varied chemical composition of these networks.[24] In a previous study, we could show that the introduction of digestible germanium nodes in one of the building blocks of POPs can also be used for partial disruption of the framework and therefore causing a decrease or allow tuning of the porosity.[25] In another approach, we introduced a poly(disulfide) hypercrosslinked polymer, which can be surface modified using unreacted thiol functions on the surface of the material.[26] Digestion of the samples helped to quantify the functionalisation. Employing digestible crosslinker or nodes is an attractive approach to gain insight into the structure or functionalisation

[a]Institute of Organic Chemistry (IOC), Karlsruhe Institute of Technology (KIT), Fritz-Haber-Weg 6, 76131 Karlsruhe, Germany. E-mail: manuel.tsotsalas@kit.edu

[b]3DMM2O – Cluster of Excellence (EXC-2082/1-390761711), Karlsruhe Institute of Technology (KIT), Kaiserstraße 12, 76131 Karlsruhe, Germany

[c]Institute of Functional Interfaces (IFG), Karlsruhe Institute of Technology (KIT), Hermann-von-Helmholtz-Platz 1, 76344 Eggenstein-Leopoldshafen, Germany

[d]Institute of Biological and Chemical Systems (IBCS-FMS), Karlsruhe Institute of Technology (KIT), Hermann-von-Helmholtz-Platz 1, 76344 Eggenstein-Leopoldshafen, Germany

† Electronic supplementary information (ESI) available. See DOI: 10.1039/d1ra05265a

‡ These authors contributed equally to this work.

of the frameworks. However, it requires the destruction of the sample and does not allow to modulate or tune the crosslinking degree reversibly in one particular system.

In order to tune and at the same time follow the crosslinking degree in porous polymer materials, we introduce the reversible multi-fold nitroxide exchange reaction to the synthesis of POPs. The nitroxide exchange reaction has been used in material science for self-assembly of polymer materials[27] or micron-sized crystals,[28] for surface functionalisation,[29] or introducing self-healing properties to materials.[30] In addition, the combination of light-sensitive alkoxyamines was employed in surface coating[31] or the creation of systems out of their equilibrium.[32] The radical nature of the involved nitroxide species allows to follow the progress of the reaction and to directly determine the crosslinking degree of the final material using fluorescence spectroscopy[33,34] and electron paramagnetic resonance (EPR) spectroscopy.[35,36] The dynamic nature of the nitroxide exchange reaction allowed us to tune the crosslinking degree of the materials by varying the ratio of the two nitroxide species involved in the reaction and thereby modulating the equilibrium conditions (see Fig. 1).

Next to the crosslinking degree, also the structure, rigidity, and the intrinsic free volume of the molecular components of POPs or CMPs play an important role to obtain porosity in the final material.[6] Cooper and co-workers showed the importance of monomer design for the pore size and surface area of CMPs by systematically varying the strut length in a series of molecular building blocks.[37]

In order to study the influence of both the molecular structure and the crosslinking degree on the porosity of the final material, we produced three different POPs based on the combination of linear, trigonal, and tetrahedral alkoxyamines with tetrahedral nitroxides. We characterised the frameworks using EPR spectroscopy and argon gas adsorption measurements to determine the crosslinking degree and porosity. Furthermore, we could show that modulating the equilibrium in the nitroxide exchange reaction, by adding or removing one nitroxide species, leads to changes in the crosslinking degree and investigated this influence on the porosity of the frameworks.
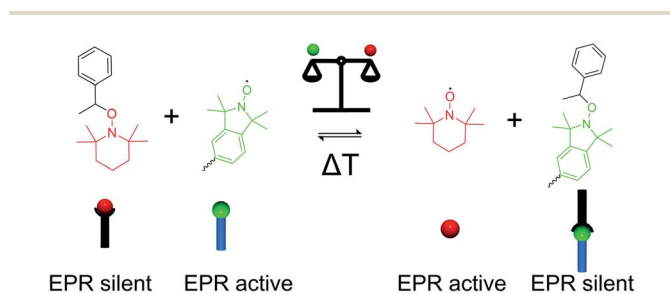
Results and discussion

The formation of POPs, with free internal volume, using the nitroxide exchange reaction requires rigid, molecular building blocks,[38,39] therefore we designed molecular building blocks in linear, trigonal, and tetrahedral geometry.[40] Fig. 2 shows the molecular structures of the di-fold, tri-fold, and tetra-fold alkoxyamines **1**–**3**, and the tetra-fold nitroxide **4**. Combinations of the alkoxyamines **1**, **2**, and **3** respectively with the nitroxide **4** lead to the frameworks by combining linear and tetrahedral [2+4], trigonal and tetrahedral [3+4], and tetrahedral and tetrahedral [4+4] geometries.

The nitroxide exchange reaction is based on the heat-induced reversible cleavage of the C–O bond of an alkoxyamine which, in this case starting from alkoxyamines **1**, **2**, and **3** leads to the persistent nitroxide radical TEMPO (**5**) and multi-fold transient C-centred radicals. These transient C-centred radicals can spontaneously form new bonds with the tetra-fold nitroxide **4**, which enable the formation of polymeric framework structures [2+4], [3+4], and [4+4]. All synthesised frameworks were obtained as insoluble powders in a yield of 20% to 47%, which were characterised using IR spectroscopy, X-ray diffraction (XRD), and scanning electron microscopy (SEM) (for synthetic details and characterisation see ESI†). SEM analysis revealed a complex topology of packed particles in the polymeric frameworks (see Fig. S1 in the ESI†). The particle size varied between 20 nm and 150 nm with free spaces in the nanometre and micrometre range. X-ray diffraction for all frameworks shows no evidence for characteristic reflections from a crystalline phase.

We determined the crosslinking degree and porosity of all synthesised polymeric frameworks by solid-state EPR spectroscopy and by sorption analyses using argon at 87 K from which the Brunauer–Emmett–Teller (BET) surface area was calculated. In Fig. 3, the EPR spectra and argon adsorption isotherms of all synthesised frameworks are shown.

The crosslinking degree of the synthesised frameworks can be straightforwardly determined from EPR data since all alkoxyamine moieties are EPR silent and the cleaved TEMPO nitroxides (**5**) are removed through washing. Therefore, the only
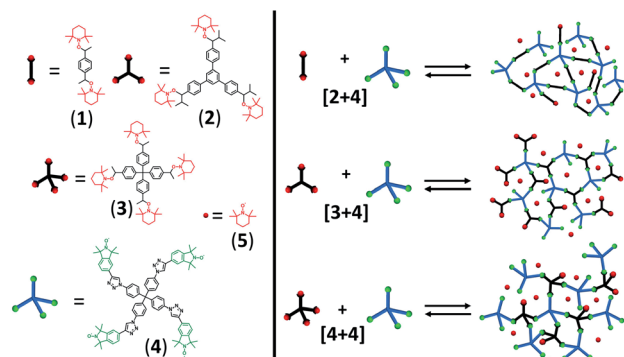

Fig. 1 Dynamic equilibrium in the nitroxide exchange reaction using two different nitroxide species, TEMPO (red) and isoindoline (green). The free nitroxide radical species are electron paramagnetic resonance (EPR) active, while the bound species are EPR silent.

Fig. 2 Molecular structures and schematic representation of the [2+4], [3+4] and [4+4] organic framework synthesized *via* nitroxide exchange reaction.
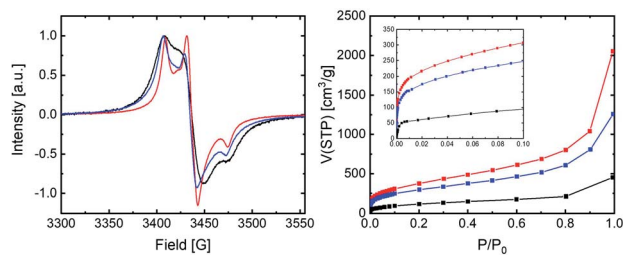
Fig. 3 Solid state EPR spectra and argon gas adsorption isotherms for the frameworks: [2+4] (black), [3+4] (red), [4+4] (blue).

EPR active moiety within the synthesised frameworks are defect sites where free isoindoline nitroxides of compound **4** are present (see again Fig. 1 for EPR active and EPR silent species). The defect density is directly represented by the measured spin density of the framework and can be used for the calculation of the crosslinking degree (CLD) of the framework.[36]

The argon adsorption isotherms of all synthesised frameworks show a sharp uptake between 10^{-5} to 2×10^{-2} P/P_0, which indicates the presence of micropores. The amount of adsorbed argon gas increased in the $P/P_0 > 0.8$ regions rapidly, which indicates the capillary condensation of macropores and mesopores within the frameworks (see Fig. 3). The BET surface areas of [2+4], [3+4], and [4+4] frameworks amount to 378 m² g⁻¹, 1200 m² g⁻¹, and 923 m² g⁻¹, respectively. All polymeric frameworks gave rise to type IV argon sorption isotherms according to IUPAC classifications.[41] Fig. 4 shows the quenched solid-state functional theory (QSDFT) pore size distribution curves for all synthesised frameworks.

The size of the pores, which make up the largest part of the porosity in the different frameworks, are in the order: [2+4] > [3+4] > [4+4]. To determine the reason for this behaviour, we compared the node-to-node strut lengths in the simulated 3D structure of each framework.[37] For the [2+4] framework, the strut length was determined to be 33.6 Å. The [3+4] framework has a strut length of 19.8 Å and the [4+4] framework a strut length of 17.5 Å. In all cases, we observed smaller micropores than the simulated strut length, which indicates a closer packing, entanglements, or catenations within the materials. Table 1 summarises the CLD, BET surface area, node-to-node strut length, and pore width of the different frameworks.
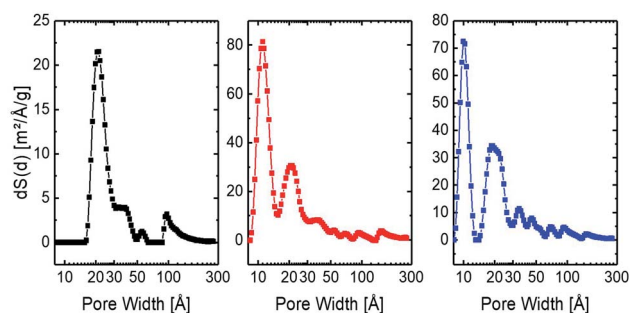
Table 1 Crosslinking degree (CLD), BET surface area, and simulated node-to-node strut length from each framework

	CLD [%]	SA_{BET} [m² g⁻¹]	L_{strut} [Å]	Pore width [Å]
[2+4]	93.4	378	33.6	21
[3+4]	94.1	1200	19.8	11
[4+4]	92.8	923	17.5	10

The reversible and dynamic nature of the nitroxide exchange reaction allows to reorganise the connectivity in the polymeric framework. Besides, the addition or removal of the TEMPO nitroxide allows us to modulate the reaction equilibrium and therefore the crosslinking degree of the frameworks (see Fig. 5).

In order to increase the CLD, by shifting the equilibrium to the product side, the synthesised frameworks were washed with toluene, until no TEMPO nitroxide was detectable in the EPR spectra of the washing solutions. Afterwards, the framework was annealed at 100 °C in dry toluene for 24 h. We could confirm the further crosslinking of the frameworks *via* EPR spectroscopy of the solid materials and the washing solutions after annealing. The washing solution of all annealed frameworks showed the presence of TEMPO nitroxides, which indicates that a fraction of previously unreacted alkoxyamine moieties in the pristine states have now reacted. Furthermore, the EPR spectra of the annealed frameworks show a decreased signal intensity in all cases, indicating a higher crosslinking degree. After characterisation of the annealed frameworks, they were de-crosslinked back to the starting material side by adding free TEMPO nitroxide and heating again to 100 °C in toluene for 24 h. Table 2 summarises the crosslinking degree and surface areas of frameworks [2+4], [3+4], and [4+4] at pristine, annealed, and de-crosslinked states.

Our results clearly show that changing the equilibrium conditions can be used to tune the crosslinking degree in porous organic frameworks (POFs) synthesised *via* nitroxide exchange reaction. However, a direct correlation of the crosslinking degree with the porosity of the system is not feasible in a straightforward fashion. While the pore size distribution shows a uniform trend, where the pore size increased for all three frameworks after annealing and decreased after de-crosslinking, the BET surface area does not show the same correlation in all systems. While the BET surface area of the framework [2+4] increases from 378 m² g⁻¹ to 666 m² g⁻¹ in the annealing step and then decreases in the de-crosslinking step to

Fig. 4 Pore size distribution of [2+4] (black), [3+4] (red), and [4+4] (blue) frameworks using the QSDFT as model.
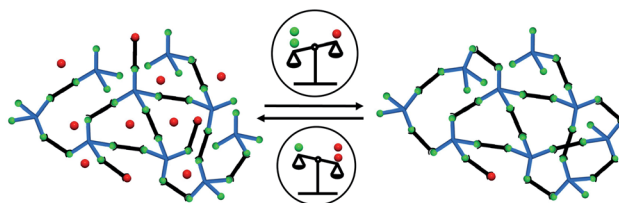

Fig. 5 Tuning of crosslinking degree *via* equilibrium control in the nitroxide exchange reaction.

Table 2 Crosslinking degrees and surface areas of [2+4], [3+4], [4+4] frameworks at pristine, annealed, and de-crosslinked states

	Pristine	Annealed	De-crosslinked
[2+4]	93.4% 378 m^2 g^{-1}	96.9% 666 m^2 g^{-1}	85.6% 260 m^2 g^{-1}
[3+4]	94.1% 1200 m^2 g^{-1}	95.4% 995 m^2 g^{-1}	86.7% 595 m^2 g^{-1}
[4+4]	92.8% 920 m^2 g^{-1}	94.8% 675 m^2 g^{-1}	88.9% 207 m^2 g^{-1}

260 m^2 g^{-1}, the other two frameworks show a different trend. The BET surface area of the [3+4] framework continuously decreases from 1200 m^2 g^{-1} to 995 m^2 g^{-1} in the annealing step and 595 m^2 g^{-1} in the de-crosslinking step. Similarly, the BET surface area of the [4+4] framework decreases from 920 m^2 g^{-1} in the pristine state to 675 m^2 g^{-1} in the annealed and then to 207 m^2 g^{-1} in the de-crosslinked state. Fig. S2 and S3† show the argon sorption isotherms and pore size distributions of all samples in a pristine, annealed, and de-crosslinked state. Our findings demonstrate that, next to the building block design, also the crosslinking degree plays an important role for the final porosity of the system. Besides, other factors such as the potential collapse of the pores, interpenetration, or surface barriers need to be considered, which can explain the observed correlations in CLD and surface areas. The findings herein can be generalised to other POF or CMP systems highlighting the importance of the reaction conditions in the final porosity of the frameworks.

Conclusion

In this work, we introduced the nitroxide exchange reaction for the synthesis of porous organic polymers. The frameworks consist of a series of linear, trigonal, and tetrahedral alkoxyamines combined with a tetrahedral nitroxide leading to frameworks [2+4], [3+4], and [4+4]. EPR spectroscopy allowed us to determine the crosslinking degree in a straightforward manner. By modulating the equilibrium conditions in the nitroxide exchange reaction, we were able to tune the crosslinking degree and thereby study the effect of the crosslinking degree on the porosity.

In our study, we found that both the crosslinking degree as well as the molecular building blocks strongly influence the porosity of the final materials. The microporosity and the pore size are strongly affected by the choice of the molecular building blocks. The combinations of trigonal and tetrahedral alkoxyamines with the tetrahedral nitroxide result in a material with a higher surface area compared to the combination of a linear alkoxyamine with the tetrahedral nitroxide. However, the crosslinking degree has a strong influence on the porosity, roughly doubling the BET surface area in the [2+4] case when going from a lower (93%) to a higher (97%) crosslinking degree. By again changing the reaction equilibrium, we could reversibly change the crosslinking degree from 97% to 86%, leading to roughly one-third of the initial porosity. However, next to the crosslinking degree also other factors need to be considered such as surface barriers or potential collapse due to the annealing procedures as evidenced in the [3+4] and [4+4]

systems where the porosity continuously decreases during annealing and de-crosslinking. We can therefore conclude that further investigations looking at structure–property relationships in CMP or POP materials need to simultaneously consider the molecular building blocks, the synthetic conditions, and the crosslinking degree, which will fundamentally facilitate the design of desired properties in these materials.

Author contributions

Isabelle Wessely: validation, investigation, resources, data curation, writing – original draft, Yannick Matt: validation, investigation, resources, data curation, writing – review and editing, Qi An: validation, investigation, resources, data curation, Stefan Bräse: conceptualization, supervision, funding acquisition. Manuel Tsotsalas: conceptualization, writing – original draft, visualization, supervision, funding acquisition.

Conflicts of interest

There are no conflicts to declare.

Acknowledgements

Notes and references

1 T. Zhang, G. Xing, W. Chen and L. Chen, Porous organic polymers: a promising platform for efficient photocatalysis, *Mater. Chem. Front.*, 2020, **4**, 332–353.
2 S. Das, P. Heasman, T. Ben and S. Qiu, Porous Organic Materials: Strategic Design and Structure–Function Correlation, *Chem. Rev.*, 2017, **117**, 1515–1563.
3 H. Bildirir, V. G. Gregoriou, A. Avgeropoulos, U. Scherf and C. L. Chochos, Porous organic polymers as emerging new materials for organic photovoltaic applications: current status and future challenges, *Mater. Horiz.*, 2017, **4**, 546–556.
4 J.-S. M. Lee and A. I. Cooper, Advances in Conjugated Microporous Polymers, *Chem. Rev.*, 2020, **120**, 2171–2214.
5 A. G. Slater and A. I. Cooper, Function-led design of new porous materials, *Science*, 2015, **348**, aaa8075.
6 Z. Hassan, Y. Matt, S. Begum, M. Tsotsalas and S. Bräse, Assembly of Molecular Building Blocks into Integrated Complex Functional Molecular Systems: Structuring Matter Made to Order, *Adv. Funct. Mater.*, 2020, **30**, 1907625.
7 R. Dawson, A. I. Cooper and D. J. Adams, Nanoporous organic polymer networks, *Prog. Polym. Sci.*, 2012, **37**, 530.

8 Y. Luo, M. Ahmad, A. Schug and M. Tsotsalas, Rising Up: Hierarchical Metal–Organic Frameworks in Experiments and Simulations, *Adv. Mater.*, 2019, **31**, 1901744.

9 S. Wuttke, D. D. Medina, J. M. Rotter, S. Begum, T. Stassin, R. Ameloot, M. Oschatz and M. Tsotsalas, Bringing Porous Organic and Carbon-Based Materials toward Thin-Film Applications, *Adv. Funct. Mater.*, 2018, **28**, 1801545.

10 P. Lindemann, A. Schade, L. Monnereau, W. Feng, K. Batra, H. Gliemann, P. Levkin, S. Bräse, C. Wöll and M. Tsotsalas, Surface functionalization of conjugated microporous polymer thin films and nanomembranes using orthogonal chemistries, *J. Mater. Chem. A*, 2016, **4**, 6815.

11 P. Lindemann, M. Tsotsalas, S. Shishatskiy, V. Abetz, P. Krolla-Sidenstein, C. Azucena, L. Monnereau, A. Beyer, A. Gölzhäuser, V. Mugnaini, H. Gliemann, S. Bräse and C. Wöll, Preparation of Freestanding Conjugated Microporous Polymer Nanomembranes for Gas Separation, *Chem. Mater.*, 2014, **26**, 7189–7193.

12 Q. An, Y. Hassan, X. Yan, P. Krolla-Sidenstein, T. Mohammed, M. Lang, S. Bräse and M. Tsotsalas, Fast and efficient synthesis of microporous polymer nanomembranes *via* light-induced click reaction, *Beilstein J. Org. Chem.*, 2017, **13**, 558.

13 D. Wu, F. Xu, B. Sun, R. Fu, H. He and K. Matyjaszewski, Design and Preparation of Porous Polymers, *Chem. Rev.*, 2012, **112**, 3959.

14 T.-X. Wang, H.-P. Liang, D. A. Anito, X. Ding and B.-H. Han, Emerging applications of porous organic polymers in visible-light photocatalysis, *J. Mater. Chem. A*, 2020, **8**, 7003.

15 A. P. Cote, A. I. Benin, N. W. Ockwig, M. O'Keeffe, A. J. Matzger and O. M. Yaghi, Porous, Crystalline, Covalent Organic Frameworks, *Science*, 2005, **310**, 1166–1170.

16 H. M. El-Kaderi, J. R. Hunt, J. L. Mendoza-Cortes, A. P. Cote, R. E. Taylor, M. O'Keeffe and O. M. Yaghi, Designed Synthesis of 3D Covalent Organic Frameworks, *Science*, 2007, **316**, 268–272.

17 M. G. Rabbani, A. K. Sekizkardes, Z. Kahveci, T. E. Reich, R. Ding and H. M. El-Kaderi, A 2D Mesoporous Imine-Linked Covalent Organic Framework for High Pressure Gas Storage Applications, *Chem.–Eur. J.*, 2013, **19**, 3324.

18 F. J. Uribe-Romo, J. R. Hunt, H. Furukawa, C. Klöck, M. O'Keeffe and O. M. Yaghi, A Crystalline Imine-Linked 3-D Porous Covalent Organic Framework, *J. Am. Chem. Soc.*, 2009, **131**, 4570–4571.

19 L. Stegbauer, K. Schwinghammer and B. V. Lotsch, A hydrazone-based covalent organic framework for photocatalytic hydrogen production, *Chem. Sci.*, 2014, **5**, 2789–2793.

20 C. S. Diercks and O. M. Yaghi, The atom, the molecule, and the covalent organic framework, *Science*, 2017, **355**, eaal1585.

21 H. Furukawa, K. E. Cordova, M. O'Keeffe and O. M. Yaghi, The Chemistry and Applications of Metal-Organic Frameworks, *Science*, 2013, **341**, 1230444.

22 Z. Ji, T. Li and O. M. Yaghi, Sequencing of metals in multivariate metal-organic frameworks, *Science*, 2020, **369**, 674–680.

23 S. Kitagawa, R. Kitaura and S. Noro, Functional Porous Coordination Polymers, *Angew. Chem., Int. Ed.*, 2004, **43**, 2334.

24 A. C. Uptmoor, J. Freudenberg, S. T. Schwäbel, F. Paulus, F. Rominger, F. Hinkel and U. H. F. Bunz, Reverse Engineering of Conjugated Microporous Polymers: Defect Structures of Tetrakis(4-ethynylphenyl)stannane Networks, *Angew. Chem., Int. Ed.*, 2015, **54**, 14673.

25 L. Monnereau, T. Muller, M. Lang and S. Bräse, Tunable porosity of 3D-networks with germanium nodes, *Chem. Commun.*, 2016, **52**, 571–574.

26 L. Monnereau, M. Nieger, T. Muller and S. Bräse, Tetrakis-(4-thiyphenyl)methane: Origin of a Reversible 3D-Homopolymer, *Adv. Funct. Mater.*, 2014, **24**, 1054.

27 H. Otsuka, Reorganization of polymer structures based on dynamic covalent chemistry: polymer reactions by dynamic covalent exchanges of alkoxyamine units, *Polym. J.*, 2013, **45**, 879–891.

28 B. Schulte, M. Tsotsalas, M. Becker, A. Studer and L. De Cola, Dynamic Microcrystal Assembly by Nitroxide Exchange Reactions, *Angew. Chem., Int. Ed.*, 2010, **49**, 6881–6884.

29 H. Wagner, M. K. Brinks, M. Hirtz, A. Schäfer, L. Chi and A. Studer, Chemical Surface Modification of Self-Assembled Monolayers by Radical Nitroxide Exchange Reactions, *Chem.–Eur. J.*, 2011, **17**, 9107–9112.

30 Y. Jia, Y. Matt, Q. An, I. Wessely, H. Mutlu, P. Theato, S. Bräse, A. Llevot and M. Tsotsalas, Dynamic covalent polymer networks *via* combined nitroxide exchange reaction and nitroxide mediated polymerization, *Polym. Chem.*, 2020, **11**, 2502–2510.

31 M. Baron, J. C. Morris, J.-L. Clément, J. Lalevée, F. Morlet-Savary, A. Spangenberg, J.-P. Malval, O. Soppera, D. Gigmes and Y. Guillaneuf, Light-Sensitive Alkoxyamines as Versatile Spatially- and Temporally- Controlled Precursors of Alkyl Radicals and Nitroxides, *J. Am. Chem. Soc.*, 2018, **140**, 3339.

32 M. Herder and J.-M. Lehn, The Photodynamic Covalent Bond: Sensitized Alkoxyamines as a Tool To Shift Reaction Networks Out-of-Equilibrium Using Light Energy, *J. Am. Chem. Soc.*, 2018, **140**, 7647–7657.

33 T. S. Fischer, S. Spann, Q. An, B. Luy, M. Tsotsalas, J. P. Blinco, H. Mutlu and C. Barner-Kowollik, Self-reporting and refoldable profluorescent single-chain nanoparticles, *Chem. Sci.*, 2018, **9**, 4696.

34 J. P. Blinco, K. E. Fairfull-Smith, A. S. Micallef and S. E. Bottle, Highly efficient, stoichiometric radical exchange reactions using isoindoline profluorescent nitroxides, *Polym. Chem.*, 2010, **1**, 1009.

35 I. Wessely, V. Mugnaini, A. Bihlmeier, G. Jeschke, S. Bräse and M. Tsotsalas, Radical exchange reaction of multi-spin isoindoline nitroxides followed by EPR spectroscopy, *RSC Adv.*, 2016, **6**, 55715–55719.

36 Q. An, I. D. Wessely, Y. Matt, Z. Hassan, S. Bräse and M. Tsotsalas, Recycling and self-healing of dynamic

covalent polymer networks with a precisely tuneable crosslinking degree, *Polym. Chem.*, 2019, **10**, 672–678.

37 J.-X. Jiang, F. Su, A. Trewin, C. D. Wood, H. Niu, J. T. A. Jones, Y. Z. Khimyak and A. I. Cooper, Synthetic Control of the Pore Dimension and Surface Area in Conjugated Microporous Polymer and Copolymer Networks, *J. Am. Chem. Soc.*, 2008, **130**, 7710.

38 N. B. McKeown and P. M. Budd, Exploitation of Intrinsic Microporosity in Polymer-Based Materials, *Macromolecules*, 2010, **43**, 5163.

39 N. B. McKeown and P. M. Budd, Polymers of intrinsic microporosity (PIMs): organic materials for membrane separations, heterogeneous catalysis and hydrogen storage, *Chem. Soc. Rev.*, 2006, **35**, 675.

40 Y. Matt, I. Wessely, L. Gramespacher, M. Tsotsalas and S. Bräse, Rigid Multidimensional Alkoxyamines: A Versatile Building Block Library, *Eur. J. Org. Chem.*, 2021, **2021**, 239–245.

41 M. Thommes, K. Kaneko, A. V. Neimark, J. P. Olivier, F. Rodriguez-Reinoso, J. Rouquerol and K. S. W. Sing, Physisorption of gases, with special reference to the evaluation of surface area and pore size distribution (IUPAC Technical Report), *Pure Appl. Chem.*, 2015, **87**, 1051.